Renewable and Sustainable Energy Reviews 168 (2022) 112785

Contents lists available at ScienceDirect

Renewable and Sustainable Energy Reviews

journal homepage: www.elsevier.com/locate/rser

Design optimization of switched reluctance machines for performance and reliability enhancements: A review

Kaikai Diao [a], Xiaodong Sun [a,*], Gerd Bramerdorfer [b], Yingfeng Cai [a], Gang Lei [c], Long Chen [a]

[a] Automotive Engineering Research Institute, Jiangsu University, Zhenjiang, 212013, China
[b] Department of Electrical Drives and Power Electronics, Johannes Kepler University Linz, Linz, 4040, Austria
[c] School of Electrical and Data Engineering, University of Technology Sydney, NSW 2007, Australia

ARTICLE INFO

Keywords:
Electromagnetic modeling
Finite element analysis (FEA)
Lumped parameter thermal network (LPTN)
Magnetic equivalent circuit (MEC) model
Multi-objective optimization
Switched reluctance machine (SRM)
System-level optimization
Thermal modeling

ABSTRACT

Switched reluctance machines (SRMs) provide a potential candidate and a feasible solution with increased interest for industrial applications due to their simple and rigid structure without permanent magnets, low manufacturing cost, excellent power-speed characteristics, and high reliability. However, the nonlinear inductance/flux linkage characteristics caused by the double-salient structure of SRM have created the challenges like high torque ripple and vibration. To solve this problem, a significant number of research works focus on the design and optimization of SRMs. Accordingly, this paper presents an in-depth literature review on the status and potential trends of design optimization techniques for SRMs, including design theory, electromagnetic and thermal modeling methods, novel topologies, optimization classifications, and techniques for optimization efficiency and effects. Existing approaches regarding the above aspects of SRMs are extensively discussed and comprehensively summarized. In addition, some essential trends in design optimization development are presented and highlighted as future perspectives. All the highlighted insights and recommendations of this review will hopefully lead to increasing efforts toward the performance and reliability enhancements of SRMs for future applications.

1. Introduction

Over the past decades, the academic and industrial communities have witnessed a rapid development of electrical machines which have been successfully designed and applied to electric vehicles (EVs)/hybrid electric vehicles (HEVs) [1–3], aircraft/aerospace systems [4–6], energy generation systems [7–9], and energy storage device [10,11]. Among all types of electrical machines, switched reluctance machines (SRMs) are attracting increased attention due to their simple and rugged structure, the absence of permanent magnets (PMs), wide operation speed range, and low manufacturing cost [12–14]. Moreover, for industrial applications, high energy efficiency and some other specifications like high power density and low weight are required. The high-efficiency SRMs are expected to be a competitive alternative to PM machines. Thus, in order to further improve the machines' performance, design and optimization methods have gained excessive attention.

Design and optimization are two major coupled stages when developing electrical machines. The main purpose of the design stage is to find a feasible solution meeting the specifications by investigating the machine type/topology design method, material properties, and performance analysis through tools or design experience. Optimization of electrical machines aims to identify the best configuration(s) among a great number of evaluated design candidates [15,16]. With the development of metamodeling techniques and an increase in computational power, most optimization problems of electrical machines are performed by means of intelligent algorithms. A number of innovative multi-objective algorithms have been proposed and applied to machine optimization, such as genetic algorithm [17–19], particle swarm optimization [20,21], and differential evolutions [22,23].

In this paper, an attempt is made to provide a comprehensive literature survey on the methods for design optimization of SRMs encompassing various aspects of design methodologies, optimization classification and techniques, and robust approaches, thus, offering researchers and engineers the most up-to-date information on the development and progress with the design and optimization technologies for SRMs. The remaining part of this article is organized as follows. Section 2 is devoted to discussing the existing design approaches for SRMs, including the design theory, and electromagnetic and thermal modeling. Section 3 presents the various novel topologies of SRMs for performance

* Corresponding author.
E-mail address: xdsun@ujs.edu.cn (X. Sun).

https://doi.org/10.1016/j.rser.2022.112785
Received 10 July 2021; Received in revised form 17 April 2022; Accepted 10 July 2022
Available online 5 August 2022
1364-0321/

List of abbreviations

AFSRM	Axial-flux switched reluctance machine
BEM	Boundary element method
CFD	Computational fluid dynamics
DOE	Design of experiments
DRSRM	Double-rotor switched reluctance machine
DSSRM	Double-stator switched reluctance machine
EV	Electric vehicle
FEA	Finite element analysis
HESRM	Hybrid-excitation switched reluctance machine
HEV	Hybrid electric vehicle
LPTN	Lumped parameter thermal network
LSRM	Linear switched reluctance machine
MEA	More electric aircraft
MEC	Magnetic equivalent circuit
PM	Permanent magnet
RFSRM	Radial-flux switched reluctance machine
SRM	Switched reluctance machine
SRSRM	Segmented-rotor switched reluctance machine
SSSRM	Segmented-stator switched reluctance machine
STSRM	Skewed-teeth switched reluctance machine

enhancement and specific applications. Section 4 classifies the optimization methods, and then the state-of-the-art optimization strategies and techniques are investigated in Section 5. This is followed by Section 6, dedicated to ongoing and future work. The conclusive remarks are presented in Section 7.

2. Design and modeling methods for SRMs

2.1. Design theory

In this section, the foundational rules of SRMs along with some empirical design formulas of SRMs will be introduced. The flux linkage characteristics of SRMs exhibit nonlinear relations concerning the phase currents and rotor positions, as presented in Fig. 1. The 0° and 180° trends reported in Fig. 1 represent the unaligned and aligned positions of SRM respectively, which correspond to the positions of minimum and maximum inductance, respectively, as illustrated in Fig. 2. Accordingly, this inherent characteristic makes the design of SRMs exhibits many uncertainties, and most size determinations are based on empirical formulas which are associated with specific topologies in the initial design stage.

The electromagnetic torque can be calculated by

$$T_e = \frac{\partial W_{co}}{\partial \theta} \quad , \text{ and} \tag{1}$$

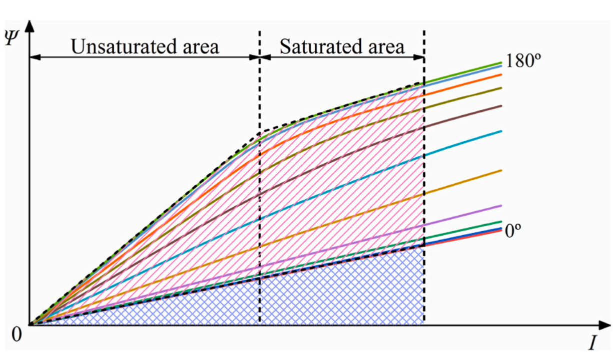

Fig. 1. Flux linkage characteristics of SRMs.

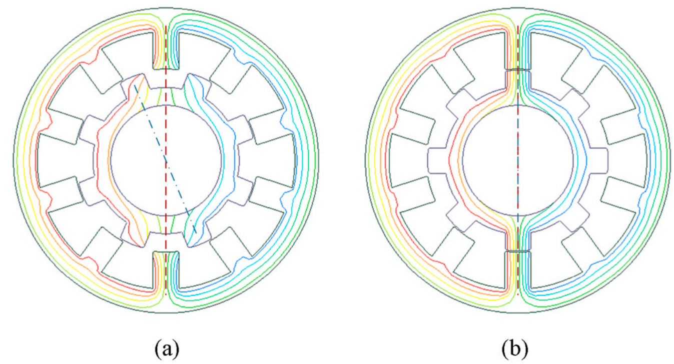

Fig. 2. (a) Unaligned and (b) aligned positions of the 10/8 SRM.

$$W_{co} = \int_0^i \psi(\theta, i)\mathrm{d}i = \int_0^i \left[L\left(\theta, i\right)i\right]di = \frac{i^2}{2}\frac{\partial L(\theta, i)}{\partial \theta} \quad , \tag{2}$$

where W_{co} is the co-energy of the field, θ and i are the rotor position and current respectively, and ψ and L are the flux linkage and inductance respectively related to θ and i. The equations indicate that the torque is proportional to the area of the conversion loop, which starts from the coordinate origin in Fig. 1 and is between the two curves of 0° and 180°. The electromagnetic torque can be qualitatively analyzed by (2). When the motor is excited in the inductance rising stage from the unaligned position to the aligned position shown in Fig. 2, the motor produces positive torque. Otherwise, braking torque will be generated.

Fig. 3 presents four representative topologies of conventional SRMs with three, four, five, and six phases. The numbers of stator and rotor poles of the conventional SRMs should follow [24]

$$Lcm(N_s, N_r) = N_{ph}N_r \tag{3}$$

where N_s, N_r, and N_{ph} represent the numbers of stator pole, rotor poles,

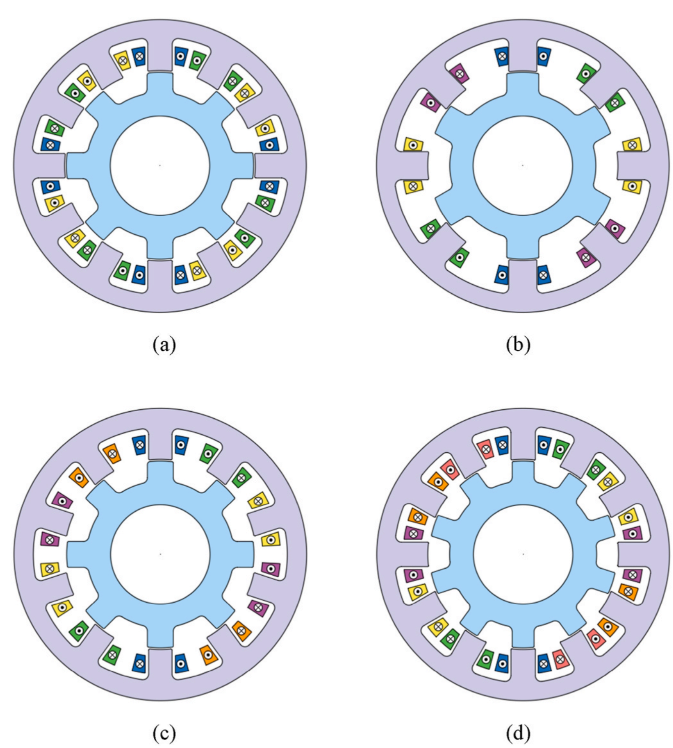

Fig. 3. Machine topologies of conventional SRMs. (a) Three-phase 12/8 SRM, (b) four-phase 8/6 SRM, (c) five-phase 10/8 SRM, and (d) six-phase 12/10 SRM.

and phase, respectively, and *Lcm* means the least common multiple.

To achieve comparable power density and efficiency with respect to other machine types, SRMs are mostly designed by making use of saturation where nonlinear characteristics have to be handled, as presented in Fig. 1. The profile sizes of the conventional SRMs are determined by the empirical formula as [25,26]

$$D^2 l = \frac{6.1}{B_\delta A} \cdot \frac{k_i}{k_m} \frac{P_{\text{em}}}{n} \tag{4}$$

where D and l are the diameter of the airgap and the stack length, respectively, k_i and k_m are the winding current coefficient and square wave current coefficient, respectively, B_δ is the magnetic load, A is the electrical load, P_{em} is the electromagnetic power, and n is the rotor speed.

2.2. Electromagnetic modeling

Accurate electromagnetic modeling provides the foundation for the subsequent optimization process. A number of studies considered the electromagnetic performances of different types of machines. These approaches can be basically classified into two categories, i.e., numerical and analytical methods.

2.2.1. Numerical methods

Numerical methods are the commonly used approach for offering a trustworthy electromagnetic solution for a variety of electrical machines considering any topology. There are two main types of numerical methods, i.e., finite element analysis (FEA), and boundary element method (BEM).

2.2.1.1. FEA. The most promising and popular numerical method is FEA [27,28]. In FEA, the analysis domain is divided into sub-regions, and each sub-region becomes a simple and small part called a finite element. In FEA, a suitable approximate solution is assumed for each element, and the solution of this domain which satisfies the conditions like the equilibrium condition of the structure is deduced. Dirichlet, Neumann, and periodic boundary conditions are applied for solving FEA problems. The definition and assignment of finite elements are flexible, which makes FEA suitable for any complex machine topologies and provides an accurate performance solution like the magnetic field distribution within any component. The computational burden is the main limit of FEA, since it needs to mesh the entire solution domain. With the increase in computational power, this problem has been gradually improved, which makes FEA the most commonly used tool. Two-dimensional (2-D) FEA instead of three-dimensional (3-D) FEA is commonly used and has become a mature technology applied for the design of SRMs [29,30]. The major deficiency of 2-D FEA is that it is generally not possible to model the variations of material properties along the axial direction, and skewing and end winding effects [31]. Consequentially, for complex topologies, especially machines with axial flux paths or skewed components, 3-D FEA provides more accurate results [32]. In addition to its application in the motor design stage, FEA is also widely used in the optimization process to, e.g., maximize the output torque and minimize the loss or ripple [33–36].

2.2.1.2. BEM. BEM is an alternative numerical method to obtain a precise magnetic solution, which also has been applied in the design optimization of SRMs [37,38]. Similar to FEA, a number of equations are assembled into a matrix form and are solved to obtain the solution. In contrast to FEA, BEM forms the boundary value problems as integral equations with boundary conditions, rather than differential equations throughout the whole design domain [39]. The main drawbacks of BEM are that the system matrix lacks symmetry and its ability to deal with nonlinear problems is poor due to the coarse treatment of anisotropic material properties. Accordingly, it is usually combined with FEA or MEC for the design and optimization of devices [39,40].

2.2.2. Analytical methods

Compared with numerical methods, analytical techniques can significantly reduce the computational effort often at the expense of accuracy. Moreover, numerical methods are unable to give a direct insight into the influence of geometrical parameters on the machine's performance, and thus the natural characteristics could not be well explained by this kind of method. In contrast, analytical techniques facilitate studying those circumstances. The main challenge of the analytical method is that it could not well approximate a complex geometry by taking an accurate evaluation of core saturation and end-winding inductance into account. The analytical methods can be classified into Maxwell's-equations-based methods, curve-fitting methods, and magnetic equivalent circuit (MEC) methods.

2.2.2.1. Maxwell's-equations-based methods. Maxwell's-equations-based methods provide magnetic field analysis by solving the partial differential equations of magnetic potentials based on Maxwell's equations [41,42]. In Ref. [43], an analytical model is developed for the unaligned inductance of the SRM. The contributions of stator and rotor slots have been accounted for. However, the stator and rotor are reshaped into rectangles for simplification, and they cannot be applied to other positions where the iron core is saturated. An enhanced model is presented in Ref. [44] to calculate the phase inductance over the full rotor position ranges. The conformal mapping is employed to calculate the permenance of the air region, and the saturation effects are considered by the combination with the MEC model. It has been proved that the slotting effects could be reduced by means of harmonic modeling and the Schwarz-Christoffel mapping method [45].

2.2.2.2. Curve-fitting methods. Curve-fitting methods approximate the models like the flux linkage or static torque with respect to rotor position and phase current. It estimates the profiles of SRM's characteristics based on a limited set of data from simulation or experiments rather than a full set of data, which can reduce the modeling cost to some extent. There are four main types of curve-fitting method, i.e., a Fourier series based approach [46–48], lookup based versions [49–51], linear/nonlinear curve-fitting formulas [52–54] and the application of the artificial intelligence method [55–58], which all have been successfully applied in SRMs.

The Fourier series based methods have been extensively used to characterize the nonlinearity of flux linkage, inductance, or torque of SRMs. The accuracy of the model typically increases with the number of considered orders. In Ref. [59], the flux-linkage models are represented by the second- and fourth-order Fourier series, respectively, as presented in Fig. 4. It can be found that in the second-order model the flux linkage at the aligned position is lower than the adjacent positions, which obey the consensus. Furthermore, the initial data used for Fig. 4 is based on the experimental results of torque-balanced positions where the static torque is zero. Thus, the cost could be greatly reduced compared with the full range of measurements.

2.2.2.3. MEC. MEC is a fast and powerful tool to provide a good compromise between computational burden and modeling accuracy. It is analogous to an electric circuit in which the electric machine is represented by a reluctance network [67]. The accuracy of MEC is mainly characterized by the level of physical geometry discretization. The reluctances of each region depend on the geometry and material permeability. The reluctance value regarding the airgap region continuously changes with the rotor position. Fig. 5 presents an MEC model for an 8/6 SRM, investigated in Ref. [66]. There are three main types of reluctance types considered in SRM, i.e., the linear reluctance with constant permeability, nonlinear reluctance decided by the material property, and reluctance changed with regard to the rotor position [62]. The slot

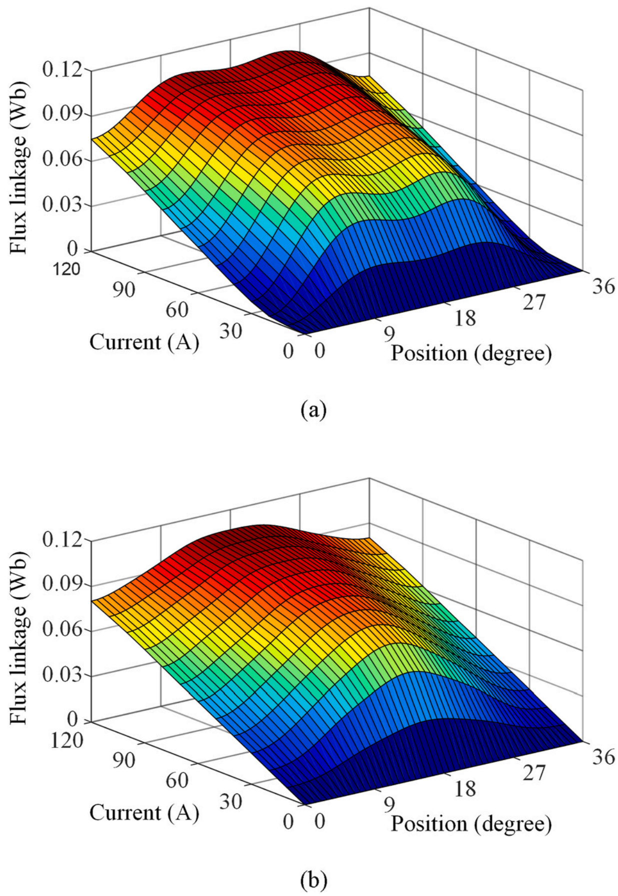

Fig. 4. Flux linkage modeling by (a) second-order and (b) fourth-order Fourier series [59].

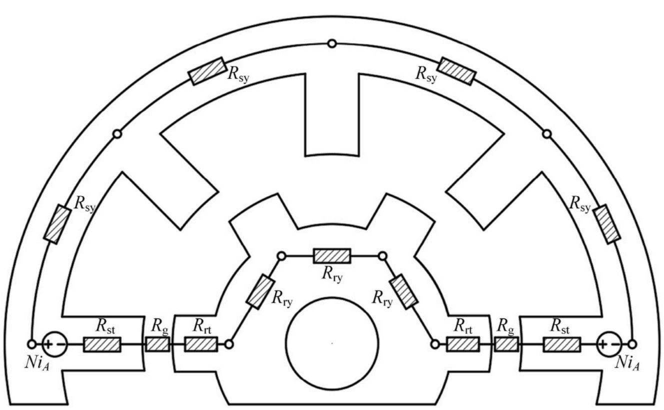

Fig. 5. MEC model of an 8/6 SRM [66].

leakage reluctance is the modeling of flux flow through the stator or rotor slot. It is determined by the stator and rotor structures and can be ignored at the aligned position. Both the stator and rotor are divided into two types of reluctance, for instance, as shown in Fig. 5, R_{sy} and R_{st} represent the reluctances of stator yoke and teeth, and R_{ry} and R_{rt} represent the reluctances of rotor yoke and teeth. The flux passing through the stator and rotor iron cores would be nonuniform with the rotation of the rotor. Therefore, more discretization of the stator and rotor region is beneficial to improve the modeling accuracy.

For better visualization and understanding, the above major electromagnetic modeling methods for SRMs are summarized in Table 1, including the classifications, advantages and disadvantages of each model.

Table 1
Summary of electromagnetic modeling for SRMs.

Classification	Modeling approach	Reference	Advantage	Disadvantage
Numerical methods	FEA	[28, 30–36]	High accuracy; can model complex structures; obtain field distributions; considers 3-D effects such as skewing and winding effects	High computational time; complex modeling process for 3-D geometry
	BEM	[37,38]	High accuracy; moderate computational time	Dense system matrix; poor ability to deal with saturation or nonlinear problems; requires to solve the boundary conditions
Analytical methods	Maxwell's-equations-based method	[41–44, 60]	Low computational time; can directly obtain the magnetic characteristics	High complexity; poor ability to deal with saturation or nonlinear problems
	Curve-fitting method	[46–53, 55–57, 61]	Low computational time; estimate the behaviours based on a limited number of data	Empirical and heuristic; require preset data; new data is required if the topology is changed
	MEC	[62–66]	Acceptable accuracy; low computational time	Empirical in assumptions of fringing/leakage reluctances; require defining flux paths in advance

2.3. Thermal modeling

The thermal analysis in the machine is significant since the life of winding and lamination insulation materials is determined by temperature rise. Moreover, the properties of materials vary with the temperature. Therefore, it is necessary for the designers to put forward a solution to balance the motor performance and heat dissipation and make full use of the cooling ability. Thermal circuit approaches and numerical techniques are two ways of approaching thermal analyses. More illustrations regarding the thermal analysis methods of electric machines can be found in Refs. [68,69].

The thermal circuit approaches rely on an equivalent lumped parameter thermal network (LPTN), where different parts of the electrical machine are modeled by lumped parameters of interconnected thermal resistors and capacitors. The network is developed by considering effects related to conduction, convection, and radiation resistances for different parts of the motor construction [70]. This approach has been widely used since it is computationally efficient and exhibits acceptable accuracy subject to the complexity of the established network. A 3-D transient LPTN conserving the axial and radial heat transfer has been proposed in Ref. [71], as shown in Fig. 6. The LPTN can solve the temperature of both interior and housing of the motor. The convection-heat-transfer coefficient is most often based on empirical formulations which are available for most of the basic geometric shapes. However, the empirical formulas may be inaccurate considering complicated motor geometries, and errors and too coarse assumptions

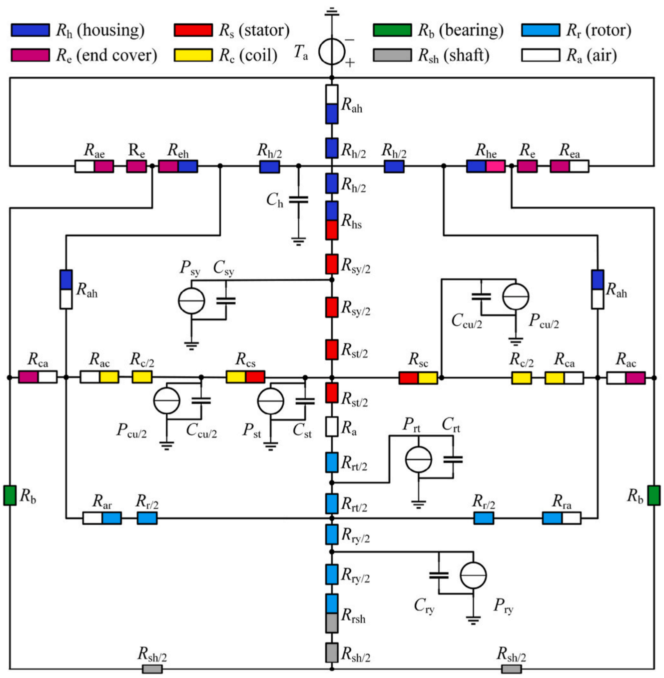

Fig. 6. 3-D LPTN of a 12/10 SRM [71].

for these coefficients can have a significant impact on model accuracy [68].

The numerical techniques mainly include FEA and computational fluid dynamics (CFD). FEA is used to model conduction in solids and predict the temperature distribution, while CFD is utilized to find the heat transfer coefficients of fluid flow for thermal circuits or FEA problems. In Ref. [72], Srinivas et al. first proposed the procedure of a flow-analysis-based thermal modeling method for SRMs, in which CFD was utilized for the evaluation of the air velocity distribution to achieve an accurate heat transfer and distribution, and FEA was conducted for the steady-state and transient thermal characteristics based on the airflow analysis. The main benefit of numerical analysis is that nearly any motor geometry can be modeled, but extended model setups and significant computation times are required [73].

The coupling between the electromagnetic and thermal fields is an essential and urgent issue in the design stage due to the strong interaction between the two aspects. The temperature rise depends on the losses obtained in the electromagnetic analysis and vice versa. Conventionally, the values and distributions of copper and iron losses are introduced into the thermal analysis as the heat source. An iteration process can be applied for the coupled analysis between the two physical fields to converge to a self-consistent solution [74]. However, it requires huge computational efforts and cannot provide real-time results for transient operations.

3. Novel design topologies

Over the past decades, conventional SRMs have been successfully designed and tested in industry applications. Moreover, various novel topologies are derived from the conventional structure for further performance and reliability improvements or some specific applications. The novel structures of SRMs can be divided into the SRMs with segmented stator/rotor [75–77], double stator/rotor [78,79], hybrid excitation [80,81], skewed teeth [82], axial flux [83], and linear structure [84,85], or the combination of the above types [86–89].

3.1. Segmented SRM

The flux path can be further shortened by incorporating the segmented parts into the SRMs. Besides, the electromagnetic isolation caused by the segmented structure can enhance the reliability and fault tolerance of the motor. The segmented SRM can be generally classified into the segmented-stator SRM (SSSRM) and the segmented-rotor SRM (SRSRM), it could also be the combination of segmented stator and segmented rotor.

There are various topologies of SSSRM, and they can be divided into SSSRM with C-core, E-core and multitooth stator according to their tooth number of segmented-stator [86,90,91]. For instance, as reported in Refs. [92,93], a novel two-phase E-core SSSRM was proposed and investigated. The stator is E-shaped with wide and narrow teeth, as presented in Fig. 7(a). Compared with the conventional two-phase SRM, the material for producing the stator core can be saved, and the iron loss can be reduced. An improved 9/12 structure was proposed in Ref. [94] which was modified to produce higher output torque. The impact of the number of segmented-stator teeth on the performance was investigated in Ref. [95], and a novel SSSRM with a multitooth stator was proposed to maximize the converted energy, as shown in Fig. 7(b).

In the literature [96], Merrow et al. presented a three-phase SRSRM with full pitch windings, as shown in Fig. 8(a). The rotor is composed of several discrete fan-shaped core blocks, embedded in the non-magnetic sleeve. The defect of this structure is that the windings span multiple stator teeth, so that the windings of different phases overlap at the end of the stator, which increases the end effects and reduces the fault tolerance. Thus, it is not suitable for applications with short axial length. To solve this problem, an SRSRM with two types of stator poles was proposed in Ref. [97]. The windings of this topology are placed around a single tooth, which occupy less copper volume compared with the full pitch SRSRM, as shown in Fig. 8(b). The performances of the SRSRMs were evaluated and compared in Ref. [98]. It was concluded that both SRSRMs with fully pitched and single-tooth windings can deliver 40% higher output torque than conventional SRM at the same copper consumption. The SRSRM with single-tooth windings would be more attractive due to its less end windings. Moreover, in Ref. [99], the SRSRMs with exciting and auxiliary stator poles were proposed and the effects of different rotor pole numbers were investigated.

3.2. Hybrid-excitation SRM

Compared with PM machines, conventional SRMs exhibit lower torque and power density. To solve this issue, one solution is to the employment of auxiliary flux sources to improve the flux density. Therefore, hybrid-excitation SRMs (HESRMs) are gaining increasing attention by adding PMs in order to improve torque production and

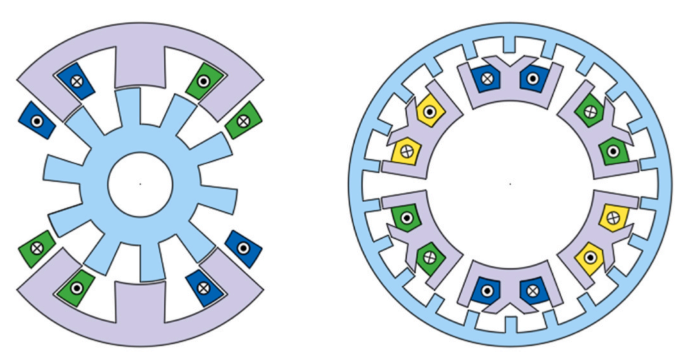

(a) (b)

Fig. 7. Machine topologies of SSSRMs with (a) E-core [92,93] and (b) multitooth stator [95].

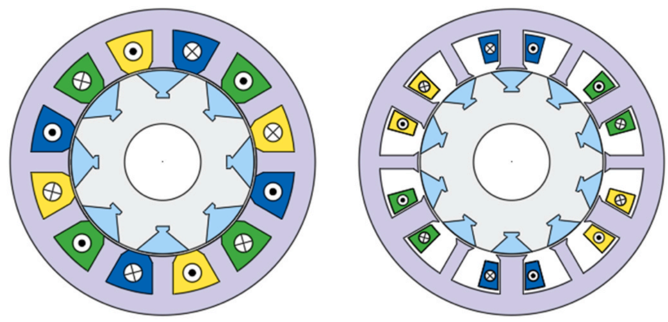

Fig. 8. Machine topologies of (a) an SRSRM with full pitch windings [96] and (b) an SRSRM with single-tooth windings [96].

power density.

In [100], a 12/8 HESRM was presented based on a C-core SSSRM, as shown in Fig. 9. By comparing it with a conventional SRM of the same size, it can be found that the HESRM has higher torque production. Furthermore, an investigation has been performed in Ref. [101] to present the influence of this topology with different pole numbers. Two HESRMs with 12/10 and 12/8 stator/rotor configurations were manufactured and comprehensively compared. The problem of such HESRM where the PMs are placed between the stator pole-tips is that the winding area is narrowed. This will influence the maximum output torque. Moreover, the heat dissipation performance gets worse. An alternative way is to arrange the PMs inside the stator teeth. However, it will cause insufficient mechanical strength [102]. Another innovative method of embedding PMs has been proposed in recent work [103]. A novel multitooth HESRM was presented where the PMs are placed between the end teeth of the adjacent modules. It can well handle the problems of the two other solutions where PMs are placed between pole-tips or inside stator teeth.

3.3. Double-stator/rotor SRM

Conventional SRMs suffer from the high vibration caused by the radial force. The double-stator SRM (DSSRM) and double-rotor SRM (DRSRM) presented in Fig. 10 provide a solution, since the electromagnetic force from the opposite directions can be offset to some extent. Besides, both the DSSRM and DRSRM have been proposed as high-power density machines [87,104,105].

The DSSRM presented in Fig. 10(a) was first introduced in Ref. [106], and the configuration including the magnetic force analysis was presented. The vibration characteristics were reported in Ref. [107] and compared with a conventional SRM. It was found that the vibration

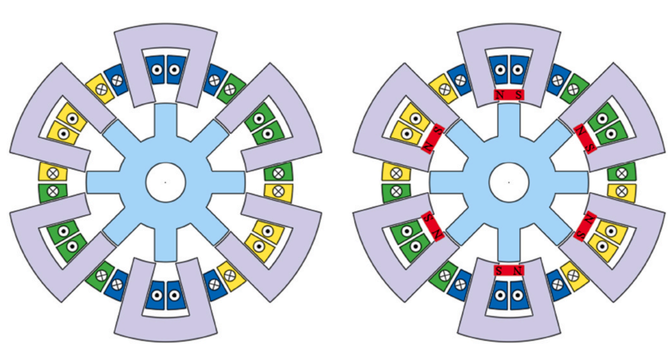

Fig. 9. Machine topologies of (a) a C-core SRM and (b) an HESRM [100].

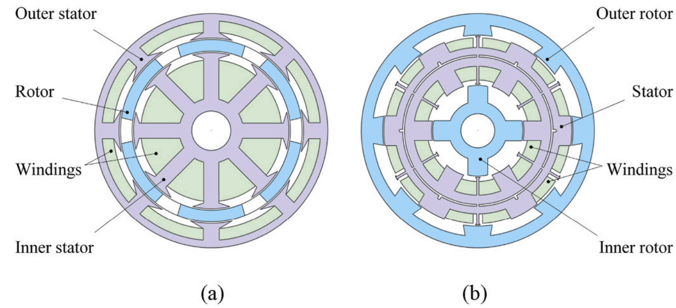

Fig. 10. Machine topologies of (a) an DSSRM [106] and (b) an DRSRM [111].

could be significantly reduced. Besides, the thermal analysis of DSSRM was performed in Ref. [104]. The design strategy including the calculation of dimensions and electromagnetic analysis of DSSRM was proposed in Ref. [108]. In Ref. [109], a novel mechanical offset DSSRM with multitooth was proposed. The two stators can provide complementary torques when teeth of the outer and inner rotor are deliberately offset by conjugate angle, hence minimizing the torque ripple. Recent works regarding the DSSRM focus on the modification and optimization of the configurations for torque ripple mitigation [35,79,110].

As reported in Ref. [78], the DRSRM was first proposed along with the working principle. Since it could provide two independent mechanical ports, DRSRM is especially suitable for HEV transmission systems where dual electromechanical energy conversion is required. A segmented rotor was incorporated into the DRSRM in Ref. [87] to improve the torque production. Based on those results, a unique DRSRM with a shared back-iron was presented in Ref. [105] for reducing the overall size. Yang et al. [111] present the detailed design procedure of the DRSRM including the analytical calculations and FEA. A novel DRSRM presented in Fig. 10(b) was designed and optimized in which both the two rotors can be controlled independently. Moreover, a family of DRSRM configurations has been introduced and compared.

3.4. Skewed-teeth SRM

Fig. 11 presents the prototypes of skewed SRM's stator and rotor. Considering the combination of skewed stator and rotor, the skewed-teeth SRM (STSRM) can be divided into three categories, the stator-only, the rotor-only, and the stator-rotor combination skewing structures. The SRMs suffer from large vibrations due to the radial magnetic force generated between the double salient poles. The benefit of the skewed topology is that it can reduce this vibration by mitigating the radial force [82].

The effects of the three types of STSRM have been investigated in Ref. [112]. It was concluded that the skewing can reduce the vibration caused by the radial pulsating force, and skewing the stator is more

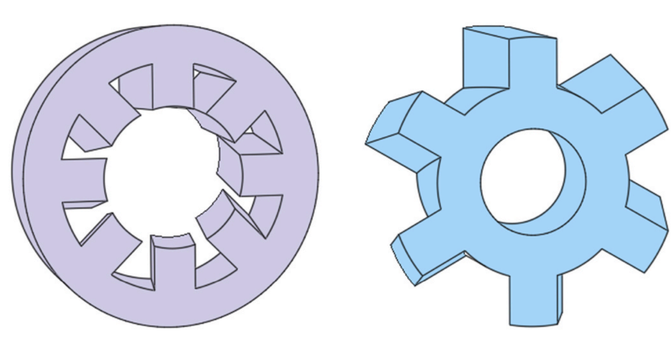

Fig. 11. Prototypes of skewed (a) stator and (b) rotor [82].

effective than skewing the rotor for vibration suppression. Moreover, skewing the stator and rotor together is the most effective way to reduce the vibration. Furthermore, in Ref. [113], the torque production of skewed-teeth SRMs was investigated and compared, and it is found that the stator-only and rotor-only skewing structures have negative effects on output torque while the stator-rotor combination skewing structure has less impact.

3.5. Axial-flux SRM

The magnetic flux lines in the airgap of the axial-flux SRM (AFSRM) are parallel to the rotation axis of the machine. It has been recognized in the literature that AFSRM exhibits higher power density than radial-flux SRM (RFSRM) due to its larger airgap surface [114]. The airgap surface of the former is dependent on the diameter of the machine whereas that of the latter is dependent on the axial length of the machine. Accordingly, AFSRM is preferred over RFSRM for applications like in-wheel motors with a high diameter to axial length ratio. The basic properties of AFSRM were presented in Ref. [115]. It has been found that the airgap length of AFSRM must be larger than that of RFSRM, since the AFSRM has a large electromagnetic force in the axial direction, which generates rotor distortion. An AFSRM with C-core stators and segmented rotors was proposed in Ref. [116], as shown in Fig. 12. It exhibits some major merits, such as higher power density, more flexible space for winding arrangement, maximized thermal dissipation, and improved fault tolerance capability.

3.6. Linear SRM

In the traditional linear motion systems, the rotary machine is usually used to drive the connecting rod to convert the rotary motion into linear motion. The overall efficiency will be affected due to the energy loss among the multistage transmission mechanism. Thus, for the vertical actuation systems, the linear machine is superior to the rotary machine in stiffness, working life, and the other performance indices. Two features should be intensively observed for the application of linear machines. One is the ratio of the payload to the onload capability, and the other is the feasibility of a long stator structure [117]. The linear induction machine and the linear synchronous machine could achieve a high respective ratio with simultaneously guaranteeing a high efficiency. However, they both have windings in the stator, which are not feasible for long-distance propulsion due to the high cost.

Linear SRM (LSRM) is an attractive alternative that has been designed and applied to rail propulsion, wave energy generation, and elevators due to its absence of PMs, concentrated rather than distributed windings, and high robustness and fault tolerance [118–120]. LSRM can be classified as a longitudinal or transverse flux type. In longitudinal LSRM, the plane of the flux is parallel to the direction of motion, while

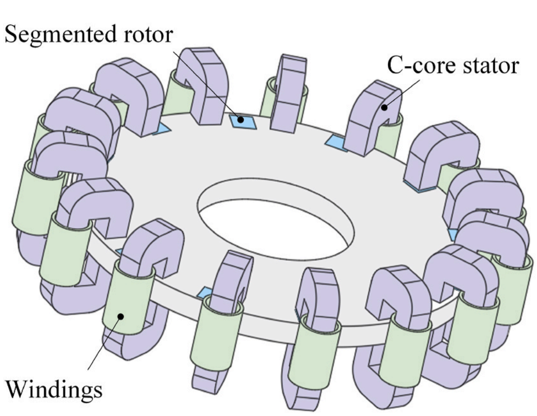

Fig. 12. Prototypes of an AFSRM [116].

that of the transverse LSRM is perpendicular to the direction of motion. The design procedure of longitudinal LSRM by converting the specifications of LSRM into the equivalent rotary SRM was proposed in Ref. [121]. Four longitudinal LSRM configurations are designed and compared in Ref. [122] for the application in vertical elevators. In addition, the electromagnetic force characteristics of a transverse LSRM were investigated in Ref. [123], and equations regarding the machines' force, efficiency, operating velocity and required voltage have been presented in Ref. [124].

In recent years, the segmented stator/translator has been adopted in LSRM. Wang et al. [117] presented the design, sensitivity analysis, and optimization of an LSRM with segmented rotors , as presented in Fig. 13(a). It was concluded that the presented LSRM exhibits high force density and copper utilization ratio, and low cost. Furthermore, the unitized design methodology for this topology has been developed in Ref. [125]. Topologies for LSRM with segmented translator were introduced in Ref. [126], and an analytical modeling has been developed for this kind of structure as illustrated in Fig. 13(b) [60].

For better visualization, in Table 2, all the above novel topologies of SRMs have been summarized and compared. The features of each topology have been clearly illustrated, and their main advantages and disadvantages have been listed.

4. Optimization classification

Optimization methods could have several forms of classification according to different criteria. Regarding the number of objectives, it could be classified into single and multi-objective optimization [134, 135]. According to whether the ontology and control variables are simultaneously optimized, it could be classified into component and system-level optimization [136]. Moreover, in terms of consideration of

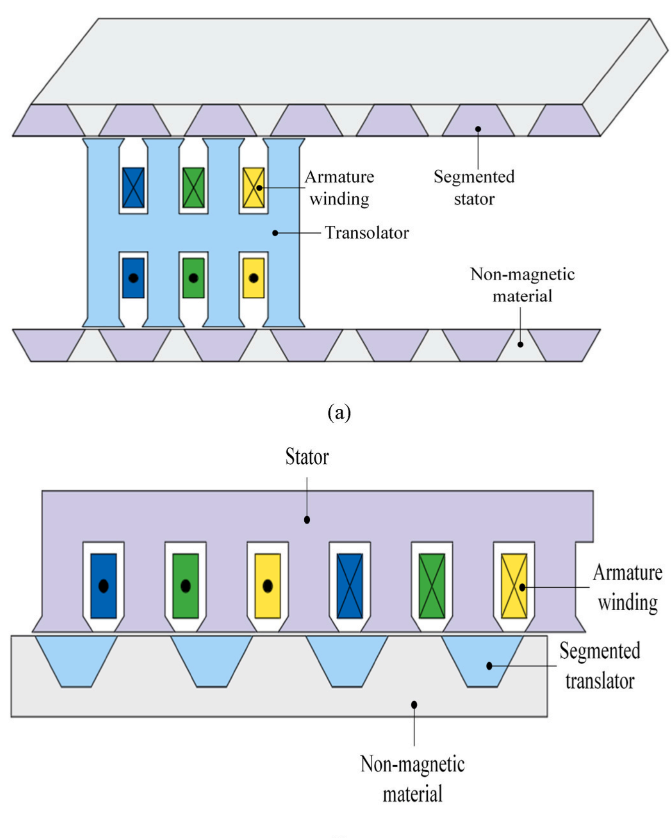

Fig. 13. Machine topologies of (a) a segmented-stator LSRM [117] and (b) a segmented-translator LSRM [60].

Table 2
Summary and comparison of various SRM topologies.

Topology	Feature	Reference	Advantages	Disadvantages
Segmented-stator SRM (SSSRM)	Adopt the segmented stator	[76,90,92–95]	Reduce iron loss; improve output torque and fault-tolerance ability	High manufacturing and assembling complexity
Segmented-rotor SRM (SRSRM)	Adopt the segmented rotor	[75,96–99,127,128]	Improve output torque; reduce windage loss and torque ripple	High manufacturing complexity; potentially mechanical weakness
Hybrid-excitation SRM (HESRM)	Add the PMs for flux enhancement	[80,100–103,129]	Improve output torque;	Insufficient mechanical strength; less inherent robustness
Double-stator SRM (DSSRM)	Assemble the rotor between the outer and inner stators	[35,79,106–110]	Reduce radial vibrations; improve energy conversion efficiency	High cost; complex structure
Double-rotor SRM (DRSRM)	Assemble the stator between the outer and inner rotors	[78,87,105,111]	Reduce radial vibration; provide two independent mechanical ports	High cost; complex structure
Skewed-teeth SRM (STSRM)	Skew the stator or rotor poles with the proper angle	[82,88,112,113]	Reduce acoustic noise and vibration; controlled with conventional schemes	Complex fabrications with different stacks between two laminations
Axial-flux SRM (AFSRM)	The magnetic flux flows along the axial direction	[114–116,130–132]	Produce high power density; suitable for applications with a high diameter to axial length ratio	High manufacturing cost
Linear SRM (LSRM)	Produce linear motion between stator and rotor	[117–122,133]	Suitable for vertical actuation systems; high fault-tolerance ability	Long stator yoke causes difficulties in the manufacturing and assembling process

uncertainties, there are deterministic and robust optimization methods [137–139].

4.1. Single and multi-objective optimization

Definition of the optimization problem is the primary and significant step of optimization. It includes the objectives, constraints, and boundaries. For single-objective optimization problems, it addresses only one performance index, which can be generally defined as

$$\begin{aligned} \text{min}:\quad & f(\mathbf{x}_s) \\ \text{s.t.}\quad & g_i(\mathbf{x}_s) \leq 0, i = 1, 2, \ldots, n \\ & \mathbf{x}_{sl} \leq \mathbf{x}_s \leq \mathbf{x}_{su} \end{aligned} \tag{5}$$

where $\mathbf{x}_s$, f, and g_i are the design parameter vector, objective and constraints of the design candidates, respectively, $\mathbf{x}_s$ consists of motor parameters and control parameters, and $\mathbf{x}_{sl}$ and $\mathbf{x}_{su}$ are the lower boundary and upper boundary, respectively.

However, the problem of single-objective optimization is that it ignores and potentially influences the other important indices. Conflicting optimization objectives are very typical such as the output torque and copper loss. Thus, the required trade-offs in multi-objective problems should be taken into consideration. Generally, a multi-objective optimization model can be defined as

$$\begin{aligned} \text{min}:\quad & \{f_1(\mathbf{x}_s), f_1(\mathbf{x}_s), \ldots, f_m(\mathbf{x}_s)\} \\ \text{s.t.}\quad & g_i(\mathbf{x}_s) \leq 0, i = 1, 2, \ldots, n \\ & \mathbf{x}_{sl} \leq \mathbf{x}_s \leq \mathbf{x}_{su} \end{aligned} \tag{6}$$

4.2. Component and system-level optimization

The operation performances of electrical machines contain two aspects, i.e., the steady-state and dynamic performances. To achieve dynamic performance, the electrical machine cooperated with control systems should be evaluated. For applications like EVs or HEVs, the energy efficiency of the whole system is more of a concern than just one component. The system-level design optimization put efforts into the selection of the best solution for the system, which provides a promising topic in recent years. The system-level optimization method for the electrical machine was first proposed in Ref. [136]. The framework of system-level optimization is presented in Fig. 14. The parameters of motor ontology and control are optimized and evaluated during the same process. It should be noted that the optimal design solution of system-level optimization aims to find the optimal system performance, but it cannot guarantee the optimal component performance like the optimal motor topology.

4.3. Deterministic and robust optimization

The deterministic optimization approach aims to provide an optimal solution or a Pareto front for electrical machines and drive systems without the consideration of uncertainties like material diversities, manufacturing tolerances, and assembly errors. It is acknowledged that manufactured products will feature inevitable deviations from the ideal model. The implementation of the deterministic approach potentially results in dissatisfying variations of output performance, especially in mass production [141].

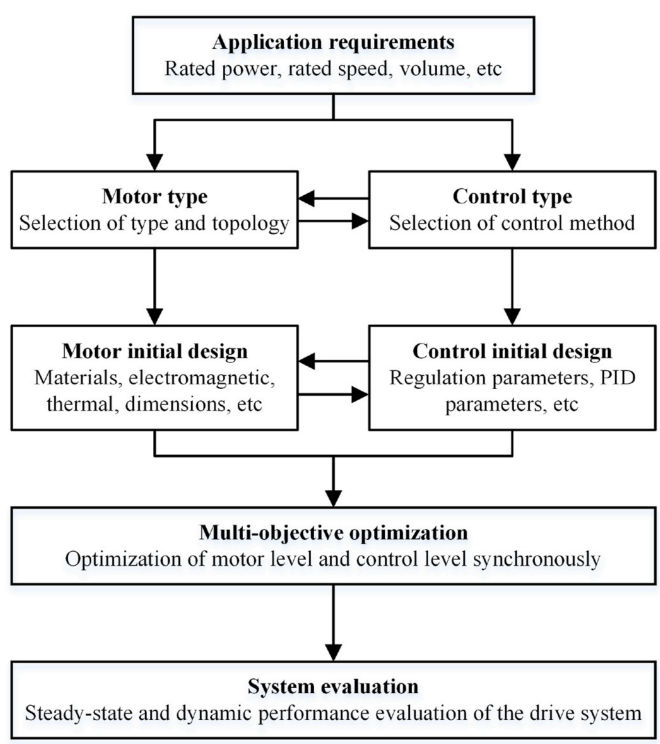

Fig. 14. A system-level optimization framework for electrical drive systems [140].

Fig. 15 presents the illustration of deterministic and robust approaches. Assume that the goal of the optimization is to minimize $f(x)$. It can be observed from Fig. 15(a) that the deterministic approach follows the overall best solution. However, when the parameter x is subject to variation within the range of Δx, the optimization objective's fluctuation of the deterministic approach is significantly larger than that of the robust approach. Moreover, some variations of solutions for the deterministic approach may exceed the constraints and become infeasible, this is forbidden in industrial applications and the rejects will increase the manufacturing cost. From Fig. 15(b), it can be seen that the robust approach achieves more concentrated design solutions within the feasible domain, while the designs of the deterministic approach are usually distributed close to the constraint boundary.

Intuitive comparisons between the deterministic and robust optimization methods can be found in Refs. [136,142]. When compared with the robust approach, a better rated performance, i.e. without considering any kind of imperfections, is typically obtained for the deterministic approach. However, the reliabilities, robustness levels, and the probability of failure are generally worse. The reliability and quality cannot be guaranteed using the deterministic approach. In Ref. [143], an example case study for PM motor optimization was investigated. It has been found that the reliabilities of the motor obtained through robust optimization are 100% which means the probability of failure of the robust approaches can be decreased to zero, while those of the deterministic designs can be lower than 30%.

5. Optimization techniques

5.1. Design of experiment (DOE)

DOE is a field of research which aims to achieve as much information as possible from a minimum number of experiments. For the design of electrical machines, the initial samples are usually generated by the DOE technique. The DOE can be classified into full factorial design and partial factor design [144]. The full factorial design is suitable for optimization problems with fewer variables, and its accuracy will be increased by the number of design levels. For example, considering a 4-factor optimization problem, $5^4 = 625$ samples and $8^4 = 4096$ are needed for the 5-level and 8-level full factorial design, respectively. The model with an 8-level full factorial design exhibits higher accuracy, but it is associated with a huge computational burden, which will greatly increase the runtime cost. In summary, the full factorial design is not suitable for high-dimensional optimization problems since it will influence the optimization efficiency and put a challenge on the computing tools. There are two solutions to solve this problem, one is the fractional factorial design, and the other is the multi-level optimization method.

5.2. Surrogate models

Surrogate models provide an alternative to FEA based evaluations for solving optimization problems specified through objectives and constraints. It is a statistical approach to global optimization by training a mathematical model on the foundation of a limited number of simulations around the operating point. It can ease the computational burden during the optimization process and has been proved as an effective way to solve the optimization with a high number of variables [145,146]. Three popular kinds of surrogate models have been widely used in the optimization problems of SRMs, namely the Kriging model [147,148], response surface model [36,149], and radial basis functions [150,151].

5.3. Multi-level optimization method

The multi-level optimization method is efficient to deal with high-dimensional optimization problems. It divides the initial design space into several low-dimensional subspaces, and the variables in each subspace are optimized sequentially. It has been proved that the multi-level optimization method provides a practically effective approach for design optimization problems to shorten the design cycle, reduce the computational cost, and improve design efficiency [152].

Fig. 16 illustrates the flowchart of the multi-level optimization method, and it has been successfully implemented for SRM in Ref. [140]. This is a high-dimensional optimization problem since the variables of the control method have been considered simultaneously as well as the structural parameters. The design variables have been divided into three subspaces according to their influence on optimization objectives, and each subspace is sequentially optimized. An iteration process has been added to the optimization process and the optimization of each subspace is performed sequentially until the convergence condition is met.

5.4. Robust optimization approach

Manufacturing imperfections and assembling errors follow inevitable deviations from the rated ideal output, which degrades the performance of the electromagnetic device. The concept of robust optimization has been illustrated in the former section. There are three popular robust optimization approaches, i.e., the Taguchi method, worst-case design, and design for six-sigma [153–156].

The worst-case design reported for the application of SRMs was presented in Ref. [153]. The reliability of the designs can be ensured by applying this method since it focuses on the worst-case performance and makes sure that it meets the requirements. In Ref. [157], a Taguchi method based approach was applied for an SRM to reduce the variability of torque and torque per inertia and meet the design requirements at the same time. The main drawback of the conventional Taguchi method is that the selection of the values and the improvement in performance is

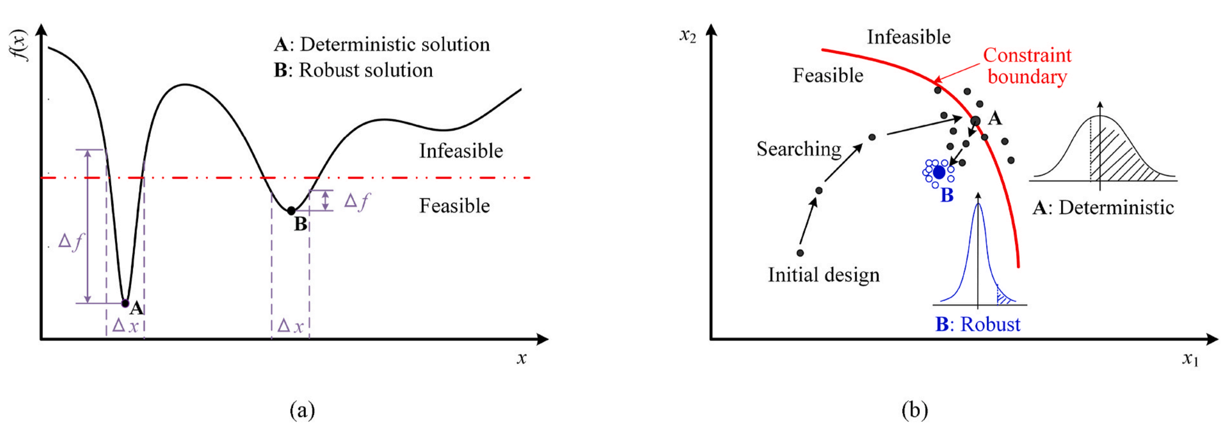

Fig. 15. Illustration of deterministic and robust optimization approaches.

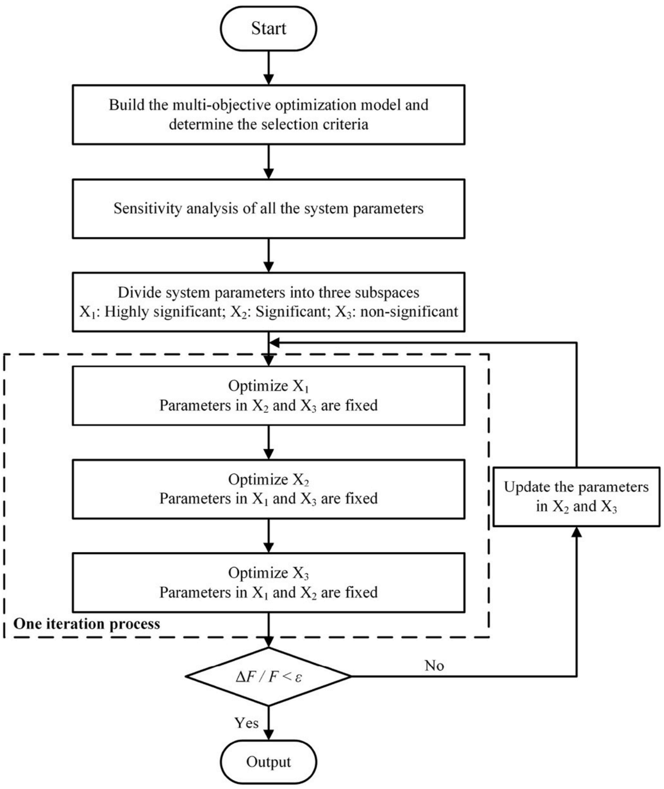

Fig. 16. Flowchart of the multi-level optimization method [140].

significantly affected by the defined levels which highly depend on the number of levels selected and the human experience. Accordingly, it has been improved in Ref. [158], in which a sequential Taguchi method was incorporated including a system-level optimization method and further a space reduction strategy was proposed for SRM drive systems. The airgap was considered in Ref. [158] as the noise factor, which very likely undergoes fluctuations during the manufacturing and assembling process. Lei et al. applied the design for the six-sigma approach for the optimization of electric machines [142,143,154], and a design example considering a PM machine was investigated. Design examples of sig-sigma on SRMs have not been reported yet.

6. Future trends

The previous sections were focusing on the design methods, novel topologies, and optimization classification and techniques. As these sections revealed, the research area of design optimization techniques for SRMs is widespread. Moreover, since PM motors take up the majority of the market share, most scholars have not emphasized SRMs [159,160]. Therefore, potential prospective research topics regarding the design optimization of SRMs exhibit great potential significance. In the following, some ideas for future trends based on the existing research experience shall be presented.

6.1. Robust topology optimization of SRMs

In general, structure optimization can be divided into three levels, namely, size, shape, and topology optimization. The size optimization aims to search for the optimal sizes of the specified components without changing the basic shape. Compared with size optimization, shape optimization is more flexible in which the geometrical parameters of the boundary points can be set as the design variables. The above two methods cannot optimize the interior domain within the boundary, for example, holes cannot arise unrestrainedly. Topology optimization aims to obtain the optimal layout of components in the prescribed design domain to obtain the best structural performance by transforming the design optimization problem into a material distribution problem [161].

Conventionally, most optimization problems are solved in a deterministic manner, known as deterministic optimization, where various sources of uncertainties are not taken into account. However, uncertainties are unavoidably observed due to the manufacturing and assembling errors, and changeable environment. They could cause great performance variations, as illustrated in Fig. 15. Therefore, there is a strongly increasing requirement to incorporate the robust optimization approach into the topology optimization for more flexible structure and sustainable reliability [162]. Robust topology optimization takes the effects of uncertainties into account for optimal topologies in structural design. It optimizes the objective performance by means of determining the ideal material distribution while simultaneously minimizing its sensitivity with respect to uncertainties. Previous works mostly focus on one side, i.e., robust or topology optimization of SRMs. For instance, in Refs. [153,155], worst-case scenario and Taguchi robust optimization have been applied in SRMs. The topology optimization method has been reported in Ref. [163] for a high-speed SRM to improve the static torque. To the authors' best knowledge, robust topology optimization method has not been reported on SRMs and even other types of electrical machines.

Robust topology optimization is an emerging topic which would be greatly suitable for SRMs to further reduce the material cost, to obtain a faster dynamic response, and to improve the cooling condition. SRMs exhibit inherent better mechanical robustness compared to motors with PMs. Thus, the topology design domain of SRMs is more flexible and more solutions can be carried out to remove the abundant materials in stator and rotor under the consideration of performance fluctuation. The main obstacles of the robust topology optimization for SRMs are the huge computational burden due to the huge number of degrees of freedom, and the coupling influence between the electromagnetic and mechanical fields. With the development of the co-simulation and metamodeling techniques, and the installation of computer clusters, such problems are evermore focused.

6.2. System-level based multidisciplinary design optimization of SRMs

In traditional design optimization works, most emphasis was put on the magnetic behaviours of SRMs, while the performances in other fields like temperature and stress are ignored. As discussed before, the life of windings and lamination materials is determined by the temperature rise, and deformation will occur due to high stress. The coupling relationships between electromagnetic, thermal, and mechanical fields should be evaluated to make full use of the performances and to ensure that the final design's performance is within the constraints. Moreover, the motors and control systems are required to be integrated as one part in the applications, and thus the evaluation of the whole drive system is more meaningful than sequentially considering the individual parts. The stable operation of SRMs is limited by the temperature rise of the power converter, and the device performance will deteriorate if the components in the power converter exceed the reasonable domain [164].

The system-level optimization of SRM has been proposed in Ref. [140], and the angle position control was investigated as the control component. Like most work, in Ref. [140], the authors superficially dealt with the thermal design aspects by determining a limiting value of current density, which does not give an insight into the temperature rise and coupling influence. In addition, it is hard to perform the system-level optimization process based on more complex control methods like direct torque control, direct instantaneous control and model predictive control due to the limited availability of appropriate tools.

The solution to consider the system-level based multidisciplinary design optimization is to apply an iteration process for the coupled analysis between the physical fields to achieve the final convergence solution [74]. This will indispensably add computational cost. Thus, it requires to derive more accurate models regarding electromagnetic, thermal and mechanical performances with low complexity and run-time, and develop more integrated software to deal with the calculation.

6.3. Application-oriented design optimization of SRMs for future transportation

From the perspective of engineering applications, the design optimization of SRMs should meet the specific requirements and constraints, such as the rated torque, the efficiency, and the given volume. Thus, the corresponding design optimization of SRMs is oriented by applications.

A great number of research efforts on SRMs have been shifted to the application of EVs and HEVs, since it has huge market potential due to the worldwide fossil fuel energy crisis and severe concluded rules regarding greenhouse gas emissions [16,165–168]. The literature gives evidence that SRMs could achieve similar performances as PM machines. For instance, an SRM machine was designed in Ref. [160] to be competitive with the interior PM synchronous machine employed in the 2009 Toyota Prius. The simulation results show that the torque, efficiency, and speed-torque region of the SRM are competitive. Load test results over the entire speed range which verify the predictions were presented in Ref. [169]. More examples could be found in Refs. [24,127, 170,171], where 50 kW, 60 kW and 80 kW SRMs are investigated and designed based on the comparison with some well-known commercial PM machines, for instance applied in the Toyota Prius or Nissan LEAF. Moreover, SRMs have been developed for in-wheel applications for small-sized EVs [34,172,173]. A 12/26 in-wheel SRSRM was prototyped in Ref. [172] to replace a brushless DC machine for providing a low-cost solution. In Ref. [173], an 18/12 in-wheel SRM was designed by utilizing a multi-objective differential evolution algorithm to satisfy the requirements. It can be found that the in-wheel SRMs are always designed with a high number of stator/rotor poles, since such configurations are beneficial to minimize vibrations, and the low-speed requirements for hub motors facilitate such configurations without requiring excessively high commutation frequencies.

Another field of future transportation is more electric aircraft (MEA). Since the early 1990s, the United States Air Force has been successfully pursuing advancements in aircraft electrical power system technologies to eliminate centralized hydraulics systems and replace them with electrical power for the improvement of aircraft weight, volume, and reliability. The concept of this process is known as MEA. In this scenario, SRMs clearly outperform PM motors or induction motors due to their superior thermal and mechanical robustness without PMs and coils in the rotor [174,175]. In aircraft systems, the SRM is mainly utilized for starter/generator applications. For instance, in Ref. [176], the SRM operates in motor mode between 900 rpm and 26,000 rpm to provide torque for accelerating the engine from light-off (maximum torque condition) to idle speed, while the machine operates in generator mode to provide electric power once the speed exceeds the idle speed. Furthermore, a 45 kW high-speed SRM was analyzed and developed as a starter/generator for an MEA system in Refs. [177,178]. Here, it was designed to realize one more function, i.e., to spin the engine through the starting sequence up to light-off speed. A novel rotor structure was developed to enlarge the speed range, and the performance during the engine-starter/motoring mode and generating mode were tested. Finally, in Ref. [179], a five-phase SRM was designed to meet the requirements of flap actuation in medium-size aircraft. The optimization approach was introduced in Ref. [180], and a comprehensive analysis and results confirming the suitability of SRMs for such applications were presented in Ref. [181].

7. Conclusion

In this paper, the state-of-the-art on design optimization of SRMs has been reviewed. First, the basic design theory, and existing electromagnetic and thermal modeling methods are presented. Then, various novel topologies of SRMs are introduced and discussed. These advanced structures have been proposed for torque enhancement, vibration reduction, or application for some scenarios featuring specific requirements. After that, optimization methods are investigated and classified according to different criteria. Several optimization methods including the design of experiments, surrogate models, and multi-level and robust optimizations, are proposed and analyzed. Finally, future perspectives of this emerging area have been pointed out, including the robust topology, system-level based multidisciplinary, and application-oriented optimization methods. Due to the inherent advantages in manufacturing cost, and thermal and mechanical robustness due to the absence of PMs, the authors believe that more SRM drives designed through applying advanced design optimization methods could take up more market share in promising applications such as EVs/HEVs, and aircraft/aerospace systems in the future.

Declaration of competing interest

The authors declare that they have no known competing financial interests or personal relationships that could have appeared to influence the work reported in this paper.

Acknowledgements

This work was supported in part by the National Natural Science Foundation of China under Project 51875261, in part by the Natural Science Foundation of Jiangsu Province of China under Project BK20180046, in part by the Postgraduate Research & Practice Innovation Program of Jiangsu Province under Project KYCX20_3014, in part by the State Scholarship Fund of China Scholarship Council under Grant 202008320572, and in part by the COMET-K2 "Center for Symbiotic Mechatronics" of the Linz Center of Mechatronics (LCM) funded by the Austrian federal government and the federal state of Upper Austria.

References

[1] Riba J-R, Lopez-Torres C, Romeral L, Garcia A. Rare-earth-free propulsion motors for electric vehicles: a technology review. Renew Sustain Energy Rev 2016;57: 367–79.
[2] Saidur R. A review on electrical motors energy use and energy savings. Renew Sustain Energy Rev 2010;14:877–98.
[3] Sun X, Wu J, Lei G, Cai Y, Chen X, Guo Y. Torque modeling of a segmented-rotor SRM using maximum-correntropy-criterion-based LSSVR for torque calculation of EVs. IEEE J Emerg Sel Top Power Electron 2021;9:2674–84.
[4] Xu Y, Zhang Z, Yu L, Shi Y. Behavior and functional modeling methods of doubly salient electromagnetic generators for aircraft electrical power system applications. Chin J Aeronaut 2019;32:477–88.
[5] Jiang X, Huang W, Cao R, Hao Z, Li J, Jiang W. Analysis of a dual-winding fault-tolerant permanent magnet machine drive for aerospace applications. IEEE Trans Magn 2015;51:1–4.
[6] Kefalas TD, Kladas AG. Thermal investigation of permanent-magnet synchronous motor for aerospace applications. IEEE Trans Ind Electron 2014;61:4404–11.
[7] Lee CHT, Chau KT, Liu C. Design and analysis of a cost-effective magnetless multiphase flux-reversal dc-field machine for wind power generation. IEEE Trans Energy Convers 2015;30:1565–73.
[8] Li J, Chau KT, Jiang JZ, Liu C, Li W. A new efficient permanent-magnet vernier machine for wind power generation. IEEE Trans Magn 2010;46:1475–8.
[9] Danikas MG, Karlis A. A review on electrical machines insulation aging and its relation to the power electronics arrangements with emphasis on wind turbine generators. Renew Sustain Energy Rev 2011;15:1748–52.
[10] Ye C, Yang J, Xu W, Xiong F, Liang X. A novel multi-unit out-rotor homopolar inductor machine for flywheel energy storage system. IEEE Trans Magn 2018;54: 1–5.
[11] Wang Q, Liu C, Zou J, Fu X, Zhang J. Numerical analysis and design optimization of a homopolar inductor machine used for flywheel energy storage. IEEE Trans Plasma Sci 2013;41:1290–4.
[12] Xu S, Chen H, Dong F, Yang J. Reliability analysis on power converter of switched reluctance machine system under different control strategies. IEEE Trans Ind Electron 2019;66:6570–80.
[13] Sun X, Wu J, Lei G, Guo Y, Zhu J. Torque ripple reduction of SRM drive using improved direct torque control with sliding mode controller and observer. IEEE Trans Ind Electron 2021;68:9334–45.

[14] Han S, Liu C, Sun X, Diao K. An effective method of verifying poles polarities in switched reluctance motors. Compel-Int J Comp Math Electr Electron Eng 2019;38:927–38.
[15] Sun X, Shi Z, Cai Y, Lei G, Guo Y, Zhu J. Driving-cycle-oriented design optimization of a permanent magnet hub motor drive system for a four-wheel-drive electric vehicle. IEEE Trans Transport Electr 2020;6:1115–25.
[16] Sun X, Diao K, Yang Z. Performance improvement of a switched reluctance machine with segmental rotors for hybrid electric vehicles. Comput Electr Eng 2019;77:244–59.
[17] Sedrine EB, Ojeda J, Gabsi M, Slama-Belkhodja I. Fault-Tolerant control using the GA optimization considering the reluctance torque of a five-phase flux switching machine. IEEE Trans Energy Convers 2015;30:927–38.
[18] Mohammadi AS, Trovão JPF, Antunes CH. Component-level optimization of hybrid excitation synchronous machines for a specified hybridization ratio using NSGA-II. IEEE Trans Energy Convers 2020;35:1596–605.
[19] Sun X, Shi Z, Lei G, Guo Y, Zhu J. Multi-objective design optimization of an IPMSM based on multilevel strategy. IEEE Trans Ind Electron 2021;68:139–48.
[20] Guo Z, Liang Y, Bian X, Wang D. Multiobjective optimization for arrangement of the asymmetric-paths winding based on improved discrete particle swarm approach. IEEE Trans Energy Convers 2018;33:1571–8.
[21] Dong F, Zhao J, Song J, Feng Y, He Z. Optimal design of permanent magnet linear synchronous motors at multispeed based on particle swarm optimization combined with SN ratio method. IEEE Trans Energy Convers 2018;33:1943–54.
[22] Zhao W, Yao T, Xu L, Chen X, Song X. Multi-objective optimization design of a modular linear permanent-magnet vernier machine by combined approximation models and differential evolution. IEEE Trans Ind Electron 2021;68(6):4634–45.
[23] Rallabandi V, Wu J, Zhou P, Dorrell DG, Ionel DM. Optimal design of a switched reluctance motor with magnetically disconnected rotor modules using a design of experiments differential evolution FEA-based method. IEEE Trans Magn 2018;54:1–5.
[24] Uddin W, Husain T, Sozer Y, Husain I. Design methodology of a switched reluctance machine for off-road vehicle applications. IEEE Trans Ind Appl 2016;52:2138–47.
[25] Song S, Zhang M, Ge L, Wang L. Multiobjective optimal design of switched reluctance linear launcher. IEEE Trans Plasma Sci 2015;43:1339–45.
[26] Hu Y, Ding W, Wang T, Li S, Yang S, Yin Z. Investigation on a multimode switched reluctance motor: design, optimization, electromagnetic analysis, and experiment. IEEE Trans Ind Electron 2017;64:9886–95.
[27] Ruuskanen V, Nerg J, Rilla M, Pyrhönen J. Iron loss analysis of the permanent-magnet synchronous machine based on finite-element analysis over the electrical vehicle drive cycle. IEEE Trans Ind Electron 2016;63:4129–36.
[28] Eit MA, Dular P, Bouillault F, Marchand C, Krebs G. Perturbation finite element method for efficient copper losses calculation in switched reluctance machines. IEEE Trans Magn 2017;53:1–4.
[29] Beltrán-Pulido A, Aliprantis D, Bilionis I, Munoz AR, Leonardi F, Avery SM. Uncertainty quantification and sensitivity analysis in a nonlinear finite-element model of a permanent magnet synchronous machine. IEEE Trans Energy Convers 2020;35:2152–61.
[30] Ding W, Hu Y, Wu L. Investigation and experimental test of fault-tolerant operation of a mutually coupled dual three-phase SRM drive under faulty conditions. IEEE Trans Power Electron 2015;30:6857–72.
[31] Yao W, Jin J, Krein PT. A highly efficient domain decomposition method applied to 3-D finite-element analysis of electromechanical and electric machine problems. IEEE Trans Energy Convers 2012;27:1078–86.
[32] Lin J, Schofield N, Emadi A. External-rotor 6-10 switched reluctance motor for an electric bicycle. IEEE Trans Transport Electr 2015;1:348–56.
[33] Chen H, Yan W, Gu JJ, Sun M. Multiobjective optimization design of a switched reluctance motor for low-speed electric vehicles with a Taguchi–CSO algorithm. IEEE ASME Trans Mechatron 2018;23:1762–74.
[34] Anvari B, Toliyat HA, Fahimi B. Simultaneous optimization of geometry and firing angles for in-wheel switched reluctance motor drive. IEEE Trans Transport Electr 2018;4:322–9.
[35] Wang W, Luo M, Cosoroaba E, Fahimi B, Kiani M. Rotor shape investigation and optimization of double stator switched reluctance machine. IEEE Trans Magn 2015;51:1–4.
[36] Ma C, Qu L. Multiobjective optimization of switched reluctance motors based on design of experiments and particle swarm optimization. IEEE Trans Energy Convers 2015;30:1144–53.
[37] Tang Y, Kline JA. Modeling and design optimization of switched reluctance machine by boundary element analysis and simulation. IEEE Trans Energy Convers 1996;11:673–80.
[38] Fauchez MB. Magnetic analysis of a switched reluctance motor using a boundary element-finite element coupling method. IEEE Trans Magn 1988;24:475–8.
[39] O'Connell TC, Krein PT. A time-harmonic three-dimensional vector boundary element model for electromechanical devices. IEEE Trans Energy Convers 2010;25:606–18.
[40] Araujo DM, Coulomb J, Chadebec O, Rondot L. A hybrid boundary element method-reluctance network method for open boundary 3-D nonlinear problems. IEEE Trans Magn 2014;50:77–80.
[41] Ilhan E, Kremers MFJ, Motoasca ET, Paulides JJH, Lomonova EA. Spatial discretization methods for air gap permeance calculations in double salient traction motors. IEEE Trans Ind Appl 2012;48:2165–72.
[42] Djelloul-Khedda Z, Boughrara K, Dubas F, Ibtiouen R. Nonlinear analytical prediction of magnetic field and electromagnetic performances in switched reluctance machines. IEEE Trans Magn 2017;53:1–11.
[43] Radun A. Analytical calculation of the switched reluctance motor's unaligned inductance. IEEE Trans Magn 1999;35:4473–81.
[44] Li S, Zhang S, Gong C, Habetler TG, Harley RG. An enhanced analytical calculation of the phase inductance of switched reluctance machines. IEEE Trans Ind Appl 2019;55:1392–407.
[45] Connell TCO, Krein PT. A Schwarz–Christoffel-based analytical method for electric machine field analysis. IEEE Trans Energy Convers 2009;24:565–77.
[46] Song S, Zhang M, Ge L. A new decoupled analytical modeling method for switched reluctance machine. IEEE Trans Magn 2015;51:1–4.
[47] Ha K, Kim R, Ramu R. Position estimation in switched reluctance motor drives using the first switching harmonics through Fourier series. IEEE Trans Ind Electron 2011;58:5352–60.
[48] Ding W, Liang D. A fast analytical model for an integrated switched reluctance starter/generator. IEEE Trans Energy Convers 2010;25:948–56.
[49] Dong J, Howey B, Danen B, Lin J, Jiang JW, Bilgin B, et al. Advanced dynamic modeling of three-phase mutually coupled switched reluctance machine. IEEE Trans Energy Convers 2018;33:146–54.
[50] Liu X, Wang C, Chen Z. Characteristics analysis of an excitation assistance switched reluctance wind power generator. IEEE Trans Magn 2015;51:1–4.
[51] Henriques LOdAP, Rolim LG, Suemitsu WI, Dente JA, Branco PJC. Development and experimental tests of a simple neurofuzzy learning sensorless approach for switched reluctance motors. IEEE Trans Power Electron 2011;26:3330–44.
[52] Xia CL, Xue M, Shi TN. A new rapid nonlinear simulation method for switched reluctance motors. IEEE Trans Energy Convers 2009;24:578–86.
[53] Chen H, Jiang D, Yang J, Shi L. A new analytical model for switched reluctance motors. IEEE Trans Magn 2009;45:3107–13.
[54] Watthewaduge G, Sayed E, Emadi A, Bilgin B. Electromagnetic modeling techniques for switched reluctance machines: state-of-the-art review. IEEE Open J Ind Electron Soc 2020;1:218–34.
[55] Huang S, Cao G, He Z, Pan JF, Duan J, Qian Q. Nonlinear modeling of the inverse force function for the planar switched reluctance motor using sparse least squares support vector machines. IEEE Trans Ind Inf 2015;11:591–600.
[56] Cai Y, Wang Y, Xu H, Sun S, Wang C, Sun L. Research on rotor position model for switched reluctance motor using neural network. IEEE ASME Trans Mechatron 2018;23:2762–73.
[57] Cao G, Chen N, Huang S, Xiao S, He J. Nonlinear modeling of the flux linkage in 2-D plane for the planar switched reluctance motor. IEEE Trans Magn 2018;54:1–5.
[58] Wu J, Sun X, Zhu J. Accurate torque modeling with PSO-based recursive robust LSSVR for a segmented-rotor switched reluctance motor. CES Trans Elect Mach Syst 2020;4:96–104.
[59] Sun X, Diao K, Lei G, Guo Y, Zhu J. Direct torque control based on a fast modeling method for a segmented-rotor switched reluctance motor in HEV application. IEEE J Emerg Sel Top Power Electron 2021;9:232–41.
[60] Golzarzadeh M, Ganji B. Analytical modelling of the linear switched reluctance motor with segmental translator. IET Electr Power Appl 2019;13:527–37.
[61] Xue XD, Cheng KWE, Ho SL, Kwok KF. Trigonometry-based numerical method to compute nonlinear magnetic characteristics in switched reluctance motors. IEEE Trans Magn 2007;43:1845–8.
[62] Sun X, Diao K, Lei G, Guo Y, Zhu J. Real-time HIL emulation for a segmented-rotor switched reluctance motor using a new magnetic equivalent circuit. IEEE Trans Power Electron 2020;35:3841–9.
[63] Sun W, Li Q, Sun L, Zhu L, Li L. Electromagnetic analysis on novel rotor-segmented axial-field SRM based on dynamic magnetic equivalent circuit. IEEE Trans Magn 2019;55:1–5.
[64] Li S, Zhang S, Dang J, Habetler TG, Harley RG. Analytical calculation of the phase inductance profile of switched reluctance machines. IEEE Trans Energy Convers 2019;34:1149–63.
[65] Yu Q, Wang X, Cheng Y. Magnetic modeling of saliency effect for saturated electrical machines with a new calculation method. IEEE Trans Magn 2016;52:1–6.
[66] Fleming FE, Edrington CS. Real-time emulation of switched reluctance machines via magnetic equivalent circuits. IEEE Trans Ind Electron 2016;63:3366–76.
[67] Taqavi O, Taghavi N. Development of a mixed solution of Maxwell's equations and magnetic equivalent circuit for double-sided axial-flux permanent magnet machines. IEEE Trans Magn 2021;57:1–11.
[68] Boglietti A, Cavagnino A, Staton D, Shanel M, Mueller M, Mejuto C. Evolution and modern approaches for thermal analysis of electrical machines. IEEE Trans Ind Electron 2009;56:871–82.
[69] Ramarathnam S, Mohammed AK, Bilgin B, Sathyan A, Dadkhah H, Emadi A. A Review of structural and thermal analysis of traction motors. IEEE Trans Transport Electr 2015;1:255–65.
[70] Dong C, Qian Y, Zhang Y, Zhuge W. A review of thermal designs for improving power density in electrical machines. IEEE Trans Transport Electr 2020;6:1386–400.
[71] Sun X, Wan B, Lei G, Tian X, Guo Y, Zhu J. Multiobjective and multiphysics design optimization of a switched reluctance motor for electric vehicle applications. IEEE Trans Energy Convers 2021;36:3294–304.
[72] Srinivas KN, Arumugam R. Analysis and characterization of switched reluctance motors: Part II. Flow, thermal, and vibration analyses. IEEE Trans Magn 2005;41:1321–32.
[73] Nasab PS, Moallem M, Chaharsoghi ES, Caicedo-Narvaez C, Fahimi B. Predicting temperature profile on the surface of a switched reluctance motor using a fast and accurate magneto-thermal model. IEEE Trans Energy Convers 2020;35:1394–401.

[74] Jiang W, Jahns TM. Coupled electromagnetic–thermal analysis of electric machines including transient operation based on finite-element techniques. IEEE Trans Ind Appl 2015;51:1880–9.
[75] Widmer JD, Mecrow BC. Optimized segmental rotor switched reluctance machines with a greater number of rotor segments than stator slots. IEEE Trans Ind Appl 2013;49:1491–8.
[76] Szabo L, Ruba M. Segmental stator switched reluctance machine for safety-critical applications. IEEE Trans Ind Appl 2012;48:2223–9.
[77] Sun X, Xue Z, Han S, Chen L, Xu X, Yang Z. Comparative study of fault-tolerant performance of a segmented rotor SRM and a conventional SRM. Bull Pol Acad Sci Tech Sci 2017;65:375–81.
[78] Shumei C, Yongjie Y, Tiecheng W. Research on switched reluctance double-rotor motor used for hybrid electric vehicle. Proc Int Conf Elect Mach Syst 2008: 3393–6.
[79] Asgar M, Afjei E. Radial force reduction in a new flat-type double-stator switched reluctance motor. IEEE Trans Energy Convers 2016;31:141–9.
[80] Lu K, Jakobsen U, Rasmussen PO. Single-phase hybrid switched reluctance motor for low-power low-cost applications. IEEE Trans Magn 2011;47:3288–91.
[81] Hwang H, Bae S, Lee C. Analysis and design of a hybrid rare-earth-free permanent magnet reluctance machine by frozen permeability method. IEEE Trans Magn 2016;52:1–4.
[82] Yang H, Lim Y, Kim H. Acoustic noise/vibration reduction of a single-phase SRM using skewed stator and rotor. IEEE Trans Ind Electron 2013;60:4292–300.
[83] Ma J, Li J, Fang H, Li Z, Liang Z, Fu Z, et al. Optimal design of an axial-flux switched reluctance motor with grain-oriented electrical steel. IEEE Trans Ind Appl 2017;53:5327–37.
[84] Jang S, Park J, Choi J, Cho H. Analytical prediction and measurements for inductance profile of linear switched reluctance motor. IEEE Trans Magn 2006; 42:3428–30.
[85] Zhao SW, Cheung NC, Gan W, Yang JM, Pan JF. A self-tuning regulator for the high-precision position control of a linear switched reluctance motor. IEEE Trans Ind Electron 2007;54:2425–34.
[86] Kondelaji MAJ, Farahani EF, Mirsalim M. Teethed-pole switched reluctance motors assisted with permanent magnets: analysis and evaluation. IEEE Trans Energy Convers 2021;36(3):2131–40.
[87] Yoshimaru Y, Higuchi T, Yokoi Y, Abe T. On the improvement performance of a dual rotor segment type SRM. Int Conf Power Electron Drive Syst 2013:1045–8.
[88] Zou Y, Cheng KE, Cheung NC, Pan J. Deformation and noise mitigation for the linear switched reluctance motor with skewed teeth structure. IEEE Trans Magn 2014;50:1–4.
[89] Pan JF, Zou Y, Cao G. An asymmetric linear switched reluctance motor. IEEE Trans Energy Convers 2013;28:444–51.
[90] Shang-Hsun M, Mi-Ching T. A novel switched reluctance motor with C-core stators. IEEE Trans Magn 2005;41:4413–20.
[91] Ding W, Hu Y, Wu L. Analysis and development of novel three-phase hybrid magnetic paths switched reluctance motors using modular and segmental structures for EV applications. IEEE ASME Trans Mechatron 2015;20:2437–51.
[92] Lee C, Krishnan R. New designs of a two-phase E-core switched reluctance machine by optimizing the magnetic structure for a specific application: concept, design, and analysis. IEEE Trans Ind Appl 2009;45:1804–14.
[93] Lee C, Krishnan R, Lobo NS. Novel two-phase switched reluctance machine using common-pole E-core structure: concept, analysis, and experimental verification. IEEE Trans Ind Appl 2009;45:703–11.
[94] Eskandari H, Mirsalim M. An improved 9/12 two-phase E-core switched reluctance machine. IEEE Trans Energy Convers 2013;28:951–8.
[95] Mousavi-Aghdam SR, Feyzi MR, Bianchi N, Morandin M. Design and analysis of a novel high-torque stator-segmented SRM. IEEE Trans Ind Electron 2016;63: 1458–66.
[96] Mecrow BC, Finch JW, El-Kharashi EA, Jack AG. Switched reluctance motors with segmental rotors. IEE Proc Elec Power Appl 2002;149:245–54.
[97] Mecrow BC, El-Kharashi EA, Finch JW, Jack AG. Segmental rotor switched reluctance motors with single-tooth windings. IEE Proc Elec Power Appl 2003; 150:591–9.
[98] Mecrow BC, El-Kharashi EA, Finch JW, Jack AG. Preliminary performance evaluation of switched reluctance motors with segmental rotors. IEEE Trans Energy Convers 2004;19:679–86.
[99] Sun X, Diao K, Lei G, Guo Y, Zhu J. Study on segmented-rotor switched reluctance motors with different rotor pole numbers for BSG system of hybrid electric vehicles. IEEE Trans Veh Technol 2019;68:5537–47.
[100] Ding W, Yang S, Hu Y, Li S, Wang T, Yin Z. Design consideration and evaluation of a 12/8 high-torque modular-stator hybrid excitation switched reluctance machine for EV applications. IEEE Trans Ind Electron 2017;64:9221–32.
[101] Ding W, Yang S, Hu Y. Development and investigation on segmented-stator hybrid-excitation switched reluctance machines with different rotor pole numbers. IEEE Trans Ind Electron 2018;65:3784–94.
[102] Masoumi M, Mirsalim M. E-core hybrid reluctance motor with permanent magnets inside stator common poles. IEEE Trans Energy Convers 2018;33: 826–33.
[103] Farahani EF, Kondelaji MAJ, Mirsalim M. An innovative hybrid-excited multi-tooth switched reluctance motor for torque enhancement. IEEE Trans Ind Electron 2021;68:982–92.
[104] Arbab N, Wang W, Lin C, Hearron J, Fahimi B. Thermal modeling and analysis of a double-stator switched reluctance motor. IEEE Trans Energy Convers 2015;30: 1209–17.
[105] Guo T, Schofield N, Emadi A. Double segmented rotor switched reluctance machine with shared stator back-iron for magnetic flux passage. IEEE Trans Energy Convers 2016;31:1278–86.
[106] Abbasian M, Moallem M, Fahimi B. Double-stator switched reluctance machines (DSSRM): fundamentals and magnetic force analysis. IEEE Trans Energy Convers 2010;25:589–97.
[107] Isfahani AH, Fahimi B. Comparison of mechanical vibration between a double-stator switched reluctance machine and a conventional switched reluctance machine. IEEE Trans Magn 2014;50:293–6.
[108] Asgar M, Afjei E, Torkaman H. A new strategy for design and analysis of a double-stator switched reluctance motor: electromagnetics, FEM, and experiment. IEEE Trans Magn 2015;51:1–8.
[109] Lee CHT, Chau KT, Liu C, Ching TW, Li F. Mechanical offset for torque ripple reduction for magnetless double-stator doubly salient machine. IEEE Trans Magn 2014;50:1–4.
[110] Gupta TD, Chaudhary K, Elavarasan RM, Saket RK, Khan I, Hossain E. Design modification in single-tooth winding double-stator switched reluctance motor for torque ripple mitigation. IEEE Access 2021;9:19078–96.
[111] Yang Y, Schofield N, Emadi A. Double-rotor switched reluctance machine (DRSRM). IEEE Trans Energy Convers 2015;30:671–80.
[112] Gan C, Wu J, Shen M, Yang S, Hu Y, Cao W. Investigation of skewing effects on the vibration reduction of three-phase switched reluctance motors. IEEE Trans Magn 2015;51:1–9.
[113] Yasa Y, Elamin M, Sozer Y, Kutz J, Tylenda JS, Wright RL. Acoustic noise mitigation for high pole count switched reluctance machines through skewing method with multiphysics FEA simulations. Proc IEEE Energy Convers Congr Expo 2017:738–44.
[114] Torkaman H, Ghaheri A, Keyhani A. Axial flux switched reluctance machines: a comprehensive review of design and topologies. IET Electr Power Appl 2019;13: 310–21.
[115] Arihara H, Akatsu K. Basic properties of an axial-type switched reluctance motor. IEEE Trans Ind Appl 2013;49:59–65.
[116] Labak A, Kar NC. Designing and prototyping a novel five-phase pancake-shaped axial-flux SRM for electric vehicle application through dynamic FEA incorporating flux-tube modeling. IEEE Trans Ind Appl 2013;49:1276–88.
[117] Wang D, Du X, Zhang D, Wang X. Design, optimization, and prototyping of segmental-type linear switched-reluctance motor with a toroidally wound mover for vertical propulsion application. IEEE Trans Ind Electron 2018;65:1865–74.
[118] Wang D, Wang X, Du X. Design and comparison of a high force density dual-side linear switched reluctance motor for long rail propulsion application with low cost. IEEE Trans Magn 2017;53:1–4.
[119] Pan JF, Zou Y, Cheung N, Cao G. On the voltage ripple reduction control of the linear switched reluctance generator for wave energy utilization. IEEE Trans Power Electron 2014;29:5298–307.
[120] Lim HS, Krishnan R, Lobo NS. Design and control of a linear propulsion system for an elevator using linear switched reluctance motor drives. IEEE Trans Ind Electron 2008;55:534–42.
[121] Byeong-Seok L, Han-Kyung B, Vijayraghavan P, Krishnan R. Design of a linear switched reluctance machine. IEEE Trans Ind Appl 2000;36:1571–80.
[122] Lobo NS, Lim HS, Krishnan R. Comparison of linear switched reluctance machines for vertical propulsion application: analysis, design, and experimental correlation. IEEE Trans Ind Appl 2008;44:1134–42.
[123] Cheng-Tsung L, Kun-Shian S, Jyh-Wei C. Operational stability enhancement analysis of a transverse flux linear switched-reluctance motor. IEEE Trans Magn 2000;36:3699–702.
[124] Baoming G, Almeida ATd, Ferreira FJTE. Design of transverse flux linear switched reluctance motor. IEEE Trans Magn 2009;45:113–9.
[125] Wang D, Zhang D, Du X, Wang X. Unitized design methodology of linear switched reluctance motor with segmental secondary for long rail propulsion application. IEEE Trans Ind Electron 2018;65:9884–94.
[126] Ganji B, Askari MH. Different topologies for linear switched reluctance motor with segmental translator. In: Proc 24th Iranian Conf Elect Eng; 2016. p. 874–8.
[127] Widmer JD, Martin R, Mecrow BC. Optimization of an 80-kW segmental rotor switched reluctance machine for automotive traction. IEEE Trans Ind Appl 2015; 51:2990–9.
[128] Sun X, Feng L, Diao K, Yang Z. An improved direct instantaneous torque control based on adaptive terminal sliding mode for a segmented-rotor SRM. IEEE Trans Ind Electron 2021;68:10569–79.
[129] Zhu J, Cheng KWE, Xue X. Design and analysis of a new enhanced torque hybrid switched reluctance motor. IEEE Trans Energy Convers 2018;33:1965–77.
[130] Labak A, Kar NC. Novel approaches towards leakage flux reduction in axial flux switched reluctance machines. IEEE Trans Magn 2013;49:4738–41.
[131] Ebrahimi Y, Feyzi MR. Introductory assessment of a novel high-torque density axial flux switched reluctance machine. IET Electr Power Appl 2017;11:1315–23.
[132] Belhadi MH, Krebs G, Marchand C, Hannoun H, Mininger X. Evaluation of axial SRM for electric vehicle application. Elec Power Syst Res 2017;148:155–61.
[133] Han-Kyung B, Byeong-Seok L, Vijayraghavan P, Krishnan R. A linear switched reluctance motor: converter and control. IEEE Trans Ind Appl 2000;36:1351–9.
[134] Yu J, Liu C. Multi-objective optimization of a double-stator hybrid-excited flux-switching permanent-magnet machine. IEEE Trans Energy Convers 2020;35: 312–23.
[135] Bramerdorfer G, Zăvoianu A. Surrogate-based multi-objective optimization of electrical machine designs facilitating tolerance analysis. IEEE Trans Magn 2017; 53:1–11.

[136] Lei G, Wang T, Guo Y, Zhu J, Wang S. System-level design optimization methods for electrical drive systems: deterministic approach. IEEE Trans Ind Electron 2014;61:6591–602.
[137] Lei G, Guo Y, Zhu J. Multidisciplinary design optimization of electrical drive systems. Springer; 2016.
[138] Bramerdorfer G, Lei G, Cavagnino A, Zhang Y, Sykulski J, Lowther DA. More robust and reliable optimized energy conversion facilitated through electric machines, power electronics and drives, and their control: state-of-the-art and trends. IEEE Trans Energy Convers 2020;35:1997–2012.
[139] Sun X, Shi Z, Zhu J. Multiobjective design optimization of an IPMSM for EVs based on fuzzy method and sequential taguchi method. IEEE Trans Ind Electron 2020;68:10592–600.
[140] Diao K, Sun X, Lei G, Guo Y, Zhu J. Multiobjective system level optimization method for switched reluctance motor drive systems using finite-element model. IEEE Trans Ind Electron 2020;67:10055–64.
[141] Bramerdorfer G. Tolerance analysis for electric machine design optimization: classification, modeling and evaluation, and example. IEEE Trans Magn 2019;55:1–9.
[142] Lei G, Wang T, Zhu J, Guo Y, Wang S. System-level design optimization method for electrical drive systems—robust approach. IEEE Trans Ind Electron 2015;62:4702–13.
[143] Lei G, Bramerdorfer G, Ma B, Guo Y, Zhu J. Robust design optimization of electrical machines: multi-objective approach. IEEE Trans Energy Convers 2021;36:390–401.
[144] Bramerdorfer G, Tapia JA, Pyrhönen JJ, Cavagnino A. Modern electrical machine design optimization: techniques, trends, and best practices. IEEE Trans Ind Electron 2018;65:7672–84.
[145] Bramerdorfer G, Zăvoianu A, Silber S, Lughofer E, Amrhein W. Possibilities for speeding up the FE-based optimization of electrical machines—a case study. IEEE Trans Ind Appl 2016;52:4668–77.
[146] Enss GC, Kohler M, Krzyżak A, Platz R. Nonparametric quantile estimation based on surrogate models. IEEE Trans Inf Theor 2016;62:5727–39.
[147] Diao K, Sun X, Lei G, Guo Y, Zhu J. Multimode optimization of switched reluctance machines in hybrid electric vehicles. IEEE Trans Energy Convers 2021;36:2217–26.
[148] Jin Z, Sun X, Cai Y, Zhu J, Lei G, Guo Y. Comprehensive sensitivity and cross-factor variance analysis-based multi-objective design optimization of a 3-DOF hybrid magnetic bearing. IEEE Trans Magn 2021;57:1–4.
[149] Neto PJdS, Barros TAdS, Paula MVd, Souza RRd, Filho ER. Design of computational experiment for performance optimization of a switched reluctance generator in wind systems. IEEE Trans Energy Convers 2018;33:406–19.
[150] Cai J, Deng ZQ, Qi RY, Liu ZY, Cai YH. A novel BVC-RBF neural network based system simulation model for switched reluctance motor. IEEE Trans Magn 2011;47:830–8.
[151] Sahraoui H, Zeroug H, Toliyat HA. Switched reluctance motor design using neural-network method with static finite-element simulation. IEEE Trans Magn 2007;43:4089–95.
[152] Lei G, Liu C, Zhu J, Guo Y. Techniques for multilevel design optimization of permanent magnet motors. IEEE Trans Energy Convers 2015;30:1574–84.
[153] Ziyan R, Zhang D, Koh C. Multi-objective worst-case scenario robust optimal design of switched reluctance motor incorporated with FEM and Kriging. Proc Int Conf Elect Mach Syst 2013:716–9.
[154] Lei G, Bramerdorfer G, Liu C, Guo Y, Zhu J. Robust design optimization of electrical machines: a comparative study and space reduction strategy. IEEE Trans Energy Convers 2021;36:300–13.
[155] Diao K, Sun X, Lei G, Bramerdorfer G, Guo Y, Zhu J. System-level robust design optimization of a switched reluctance motor drive system considering multiple driving cycles. IEEE Trans Energy Convers 2021;36:348–57.
[156] Shi Z, Sun X, Cai Y, Yang Z. Robust design optimization of a five-phase PM hub motor for fault-tolerant operation based on Taguchi method. IEEE Trans Energy Convers 2020;35:2036–44.
[157] Omekanda AM. Robust torque and torque-per-inertia optimization of a switched reluctance motor using the Taguchi methods. IEEE Trans Ind Appl 2006;42:473–8.
[158] Diao K, Sun X, Lei G, Bramerdorfer G, Guo Y, Zhu J. Robust design optimization of switched reluctance motor drive systems based on system-level sequential Taguchi method. IEEE Trans Energy Convers 2021;36:3199–207.
[159] Shi Z, Sun X, Lei G, Yang Z, Guo Y, Zhu J. Analysis and optimization of radial force of permanent-magnet synchronous hub motors. IEEE Trans Magn 2020;56:1–4.
[160] Kiyota K, Chiba A. Design of switched reluctance motor competitive to 60-kW IPMSM in third-generation hybrid electric vehicle. IEEE Trans Ind Appl 2012;48:2303–9.
[161] Zhao Q, Chen X, Ma Z-D, Lin Y. Robust topology optimization based on stochastic collocation methods under loading uncertainties. Math Probl Eng 2015;2015.
[162] Bramerdorfer G. Effect of the manufacturing impact on the optimal electric machine design and performance. IEEE Trans Energy Convers 2020:1.
[163] Zhang H, Xu W, Wang S, Huangfu Y, Wang G, Zhu J. Optimum design of rotor for high-speed switched reluctance motor using level set method. IEEE Trans Magn 2014;50:765–8.
[164] Chen H, Xu Y. Electromagnetic field analysis coupled model of fluid–structure–thermal simulation of power converter for switched reluctance machine. IEEE Trans Appl Supercond 2016;26:1–6.
[165] Sun X, Shen Y, Wang S, Lei G, Yang Z, Han S. Core losses analysis of a novel 16/10 segmented rotor switched reluctance BSG motor for HEVs using nonlinear lumped parameter equivalent circuit model. IEEE ASME Trans Mechatron 2018;23:747–57.
[166] Cheng H, Wang L, Xu L, Ge X, Yang S. An integrated electrified powertrain topology with SRG and SRM for plug-in hybrid electrical vehicle. IEEE Trans Ind Electron 2020;67:8231–41.
[167] Nguyen D, Bahri I, Krebs G, Berthelot E, Marchand C, Ralev I, et al. Efficiency improvement by the intermittent control for switched reluctance machine in automotive application. IEEE Trans Ind Appl 2019;55:4167–82.
[168] Sun X, Wu J, Wang S, Diao K, Yang Z. Analysis of torque ripple and fault-tolerant capability for a 16/10 segmented switched reluctance motor in HEV applications. Compel-Int J Comp Math Electr Electron Eng 2019;38:1725–37.
[169] Kiyota K, Kakishima T, Chiba A. Comparison of test result and design stage prediction of switched reluctance motor competitive with 60-kW rare-earth PM motor. IEEE Trans Ind Electron 2014;61:5712–21.
[170] Takeno M, Chiba A, Hoshi N, Ogasawara S, Takemoto M, Rahman MA. Test results and torque improvement of the 50-kW switched reluctance motor designed for hybrid electric vehicles. IEEE Trans Ind Appl 2012;48:1327–34.
[171] Jiang JW, Bilgin B, Emadi A. Three-phase 24/16 switched reluctance machine for a hybrid electric powertrain. IEEE Trans Transport Electr 2017;3:76–85.
[172] Nikam SP, Rallabandi V, Fernandes BG. A high-torque-density permanent-magnet free motor for in-wheel electric vehicle application. IEEE Trans Ind Appl 2012;48:2287–95.
[173] Öksüztepe E. In-wheel switched reluctance motor design for electric vehicles by using a Pareto-based multiobjective differential evolution algorithm. IEEE Trans Veh Technol 2017;66:4706–15.
[174] Li S, Zhang S, Habetler TG, Harley RG. Modeling, design optimization, and applications of switched reluctance machines—a review. IEEE Trans Ind Appl 2019;55:2660–81.
[175] Cao W, Mecrow BC, Atkinson GJ, Bennett JW, Atkinson DJ. Overview of electric motor technologies used for more electric aircraft (MEA). IEEE Trans Ind Electron 2011;59:3523–31.
[176] MacMinn SR, Jones WD. A very high speed switched-reluctance starter-generator for aircraft engine applications. In: Proceedings of the IEEE National Aerospace and Electronics Conference. 4; 1989. p. 1758–64.
[177] Bartolo JB, Gerada C. The electromagnetic design of a high speed, 45kW, switched reluctance machine having a novel rotor geometry for aerospace application. In: 2014 International Conference on Electrical Machines (ICEM); 2014. p. 2513–9.
[178] Bartolo JB, Degano M, Espina J, Gerada C. Design and initial testing of a high-speed 45-kW switched reluctance drive for aerospace application. IEEE Trans Ind Electron 2017;64:988–97.
[179] Villani M, Tursini M, Fabri G, Leonardo LD. A switched-reluctance motor for aerospace application. In: 2014 International Conference on Electrical Machines (ICEM); 2014. p. 2073–9.
[180] Castellini L, Lucidi S, Villani M. Design optimization of switched reluctance motor for aerospace application. IEEE International Electric Machines & Drives Conference (IEMDC); 2015. p. 1678–82.
[181] Tursini M, Villani M, Fabri G, Di Leonardo L. A switched-reluctance motor for aerospace application: design, analysis and results. Elec Power Syst Res 2017;142:74–83.